Soil Biology and Biochemistry 122 (2018) 60–70

Contents lists available at ScienceDirect

Soil Biology and Biochemistry

journal homepage: www.elsevier.com/locate/soilbio

Soil microbial populations in deep floodplain soils are adapted to infrequent but regular carbon substrate addition

E.L. Cressey[a,*], J.A.J. Dungait[b], D.L. Jones[c], A.P. Nicholas[a], T.A. Quine[a]

[a] College of Life and Environmental Sciences, University of Exeter, Rennes Drive, Exeter, Devon, EX4 4RJ, UK
[b] Sustainable Agriculture Sciences, Rothamsted Research, North Wyke, Okehampton, Devon, EX20 2SB, UK
[c] School of Environment, Natural Resources and Geography, Bangor University, Gwynedd, LL57 2UW, UK

ARTICLE INFO

Keywords:
Soil organic carbon
Soil microbial biomass
^{14}C-labelling
Dissolved organic carbon
Depth
Mineralisation
Floodplain
Stoichiometry

ABSTRACT

Floodplain soils provide an important link in the land-ocean aquatic continuum. Understanding microbial activity in these soils, which can be many metres deep, is a key component in our understanding of the role of floodplains in the carbon (C) cycle. We sampled the mineral soil profile to 3 m depth from two floodplain sites under long-term pasture adjacent to the river Culm in SW England, UK. Soil chemistry (C, nitrogen (N), phosphorus (P), soil microbial biomass (SMB), moisture content) and soil solution (pH, dissolved organic C (DOC) and N, nitrate, ammonium, water extractable P) were analysed over the 3 m depth in 6 increments: 0.0–0.2, 0.2–0.7, 1.0–1.5, 1.5–2.0, 2.0–2.5, and 2.5–3.0 m. ^{14}C-glucose was added to the soil and the evolution of $^{14}CO_2$ measured during a 29 d incubation. From soil properties and ^{14}C-glucose mineralisation, three depth groups emerged, with distinct turnover times extrapolated from initial k_1 mineralisation rate constants of 2 h (topsoil 0.0–0.2 m), 4 h (subsoil 0.2–0.7 m), and 11 h (deep subsoil 1.0–3.0 m). However, when normalised by SMB, k_1 rate constants had no significant differences across all depths. Deep subsoil had a 2 h lag to reach maximal $^{14}CO_2$ production whereas the topsoil and subsoil (0.2–0.7 m) achieved maximum mineralisation rates immediately. SMB decreased with depth, but only to half of the surface population, with the proportion of SMB-C to total C increasing from 1% in topsoil to 15% in deep subsoil (> 1.0 m). The relatively large SMB concentration and rapid mineralisation of ^{14}C-glucose suggests that DOC turnover in deep soil horizons in floodplains is limited by access to biologically available C and not the size of the microbial population.

1. Introduction

Carbon (C) dynamics in deep soil are some of the most poorly understood components of the global C cycle, despite an estimated 75% of the C found in the top 3 m of soil occurring below 0.2 m (Jobbágy and Jackson, 2000; Rumpel and Kögel-Knabner, 2010). Subsoil soil organic carbon (SOC) has predominantly been considered older (i.e., large radiocarbon age), more stable and chemically recalcitrant than that of topsoil (Wordell-Dietrich et al., 2017), with decomposition rates increasing with depth down the profile. However, many existing SOC decomposition models tend to simplify decay rates to one pool, which can lead to an underestimation of the amount of C observed at depth (Jenkinson and Coleman, 2008). Subsoils have been suggested as having the potential to store additional C due to reduced microbial activity at depth, but there is debate surrounding the stability of C in subsoil (Kramer et al., 2013; Jones et al., 2018). Recent studies have reported little difference in the decomposability of topsoil SOC compared with subsoil SOC, with stability potentially linked to the physical environment rather than the molecular recalcitrance of subsoil SOC (Fontaine et al., 2007; Gregory et al., 2016; Heitkötter et al., 2017; Jones et al., 2018). Subsoils vary in oxygen availability, moisture content (MC), mineralogy, metal concentrations, quantity and quality of SOC and microbial population abundance when compared to topsoil, and increasing spatial heterogeneity, i.e., physical separation of decomposers to available substrate, which may all contribute to observed stability (Salomé et al., 2010; Chaopricha and Marín-Spiotta, 2014; Wordell-Dietrich et al., 2017; Jones et al., 2018).

Deep soils are characterised by having SOC radiocarbon ages of many thousands of years (e.g. 2500 y at 0.6–0.8 m; Fontaine et al., 2007). However, rapid accretionary environments, such as floodplain soils, can be much younger (e.g. > 250 y for the top 0.6 m; Lair et al., 2009). Some floodplain soils can extend beyond 8 m in depth and the age can vary greatly depending on soil conditions (Lair et al., 2009; Zehetner et al., 2009; Chaopricha and Marín-Spiotta, 2014). Floodplains are dynamic, complex systems characterised by large spatial and temporal variation in physical and chemical characteristics, e.g. in

* Corresponding author.
E-mail address: E.Cressey@exeter.ac.uk (E.L. Cressey).

https://doi.org/10.1016/j.soilbio.2018.04.001
Received 30 June 2017; Received in revised form 26 March 2018; Accepted 2 April 2018
Available online 12 April 2018

water flow, channel migration, sediment transportation and nutrient retention (Raymond and Bauer, 2001; Graf-Rosenfellner et al., 2016). They are also productive ecosystems due to the continual input of fresh, nutrient rich sediments resetting soil formation to an early phase of OC accumulation with rapid accumulation of labile C and nitrogen (N; Zehetner et al., 2009). However, the biogeochemical processes occurring in these systems remain poorly understood.

There is debate over the survival of C in floodplain systems with Wang et al. (2014) reporting 2–14 times slower turnover of SOC in depositional areas, with buried SOC in saturated riparian soils remaining stable for thousands of years (Chaopricha and Marín-Spiotta, 2014). By contrast, Hoffmann et al. (2013) suggested rapid turnover and reduced C sequestration rates. The complexity of floodplain C dynamics is also increased by the additional lateral and vertical fluxes of C from erosion, flooding and sediment deposition (Regnier et al., 2013; Jansen et al., 2014) and by enhanced vertical movement of dissolved OC (DOC) due to flushing of C from upper soil horizons (Morel et al., 2009). Furthermore, the co-transport of nutrients is likely to affect the stoichiometry of depositional soils in favour of mineralisation. Carbon storage in deeper soils is suggested to be due to the limitation of easily available substrate (Fontaine et al., 2007; Salomé et al., 2010; Heitkötter et al., 2017; Jones et al., 2018). Indeed, microbial hotspots in deep unsaturated subsoils have been reported in areas of preferential DOC flow (Gocke et al., 2017). Therefore, riparian soils with regular inputs of DOC during flood events may have enhanced mineralisation potential in the hyporheic zone (Marín-Spiotta et al., 2014).

Carbon storage in subsoils may also be driven by the vertical transport of DOC, which is subsequently chemically protected (Kramer and Gleixner, 2008; Müller et al., 2016). Alternating redox conditions in periodically inundated soils can lead to anoxic conditions, which, in turn, can lead to reduced decomposition rates, increased SOC and DOC accumulation and increased denitrification (Bräuer et al., 2013; Hanke et al., 2013; Ding et al., 2017). Furthermore, the predicted increases in temperature and precipitation from the altering of the North Atlantic storm track and intensification of the global hydrological cycle due to climate change may alter the redox state from increased flushing and/or waterlogging (Orme et al., 2017). This might result in high intensity erosion events, changes to soil microbial activity, and may also cause enhanced nitrification, denitrification respiration, methanogenesis rates and increased DOC transport through soils (Keller and Bridgham, 2007; Beniston et al., 2015; Poblador et al., 2017).

Despite the potential significance of floodplain soils in the terrestrial C cycle, they are acknowledged to be under-represented in empirical studies (Bullinger-Weber et al., 2014). Riverine systems are dynamic and likely to become more so with future climate change, with Worrall et al. (2004) reporting an increase of 0.02 Mt C y^{-1} in the UK riverine DOC flux of 0.86 Mt C y^{-1}, and Sandford et al. (2013) reporting a 91% increase in DOC in UK rivers and lakes over the past 20 years, with the coincident increasing supplies of biologically available C and other macronutrients (e.g. N and phosphorus (P)). Therefore, it is important to measure the response of microbial activity to DOC in this largely unquantified environment. We test the hypothesis that deep floodplain soil systems support a relatively large metabolically alert microbial population able to respond rapidly to substrate supply. Our study was based on a rapidly accreting mineral soil under permanent pasture, undergoing regular flood inundation (approx. 8 times per year, with floodwaters typically receding within 24 h; Walling and Bradley, 1989; Simm and Walling, 1998; Walling et al., 2006). The hypothesis was tested using measurements of soil microbial biomass (SMB), basal respiration and the addition of a ^{14}C-labelled simple sugar (glucose) under aerobic laboratory conditions as a general proxy for microbial activity in a dynamic temperate grassland floodplain soil profile.

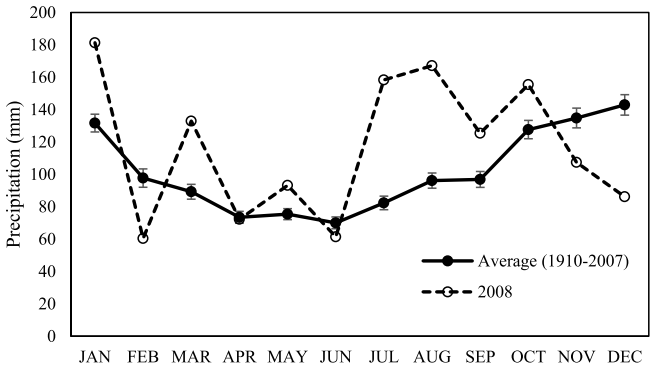

Fig. 1. Average precipitation for the SW of England and S Wales for 1910–2007 (errors are SEM) and precipitation (mm) for 2008 (data from: Met Office, 2017).

2. Materials and methods

2.1. Field sites

The field sites were two active channel riparian grassland sites (Smithincott: 50°33′50.2″ N, 3°20′34.8″ W and Rewe: 50°47′15.2″ N, 3°29′20.0″ W) on the river Culm in SW England, UK that are permanent pasture grazed by cattle in the summer. The river has a catchment of 276 km^2, with a mean altitude of 140 m a.s.l., dominated by sandstone and marl lithology, with a mean precipitation of 952 mm and an estimated sediment yield of 25 t km^{-2} y^{-1} (Walling et al., 2006). However, 2008 was a notably stormy year with elevated rainfall (Fig. 1); during which SW England experienced a 15% increase in recorded precipitation above the annual average (from 1910 to 2007), with 65% greater precipitation than average in the three months prior to sampling (Met Office, 2017).

2.2. Soil sampling

Soil cores were sampled in October 2008. At Smithincott, 7 cores were sampled along a transect perpendicular to the bank, with the primary transect 30 m from the river channel, with 4 cores sampled at 10 m intervals and a secondary transect of 3 cores 10 m perpendicular to the bank; all cores were sampled 25 m apart. At Rewe, 5 cores were sampled at 20 m intervals along a transect from 15 m from the bank to a maximum distance of 85 m from the channel.

Soil cores were extracted from 0.0 to 3.0 m depth and divided into 6 depth increments: 0.0–0.2 (n = 12), 0.2–0.7 (n = 12), 1.0–1.5 (n = 10), 1.5–2.0 (n = 10), 2.0–2.5 (n = 6) and 2.5–3.0 m (n = 6). Topsoil (0.0–0.2 m) and subsoil (0.2–0.7 m) cores were sampled using a percussion hammer (0.1 m diameter; Wacker Neuson Ltd, Stafford, UK), directly adjacent to deep subsoil cores (1.0–3.0 m), sampled using a pneumatic corer (0.03 m diameter; Geoprobe, DT22 Soil Sampling System, KS, USA) to reduce compaction effects in the top metre. The cores were sealed in plastic tubes and stored at 4 °C for 1 week prior to analysis.

As per Fontaine et al. (2007), Heitkötter et al. (2017) and Wordell-Dietrich et al. (2017), topsoil and subsoil were sieved, under aerobic conditions, prior to analysis through a large mesh (7 mm) to maintain soil aggregate structure, to homogenise the samples and remove large roots and stones. Sieving through mesh of this size does not significantly affect soil microbial activity or the intrinsic DOC dynamics of the soil (Jones and Willett, 2006). The sieved soil samples were subdivided into four equal portions for mineralisation, respiration, analyses of soil properties and soil solution extractions and stored in gas permeable bags at 4 °C.

2.3. Soil properties and soil solution characteristics

Bulk soil was further sieved through 2 mm mesh to remove roots and analysed for soil particle size, pH and total C, N and P and organic P ($P_{organic}$). Soil particle size was measured by high definition digital particle size analysis using a Saturn DigiSizer (Micromeritics, Saturn DigiSizer™ 5200, Norcross, GA, USA). Soil pH was determined in a 1:1 (*v/v*) soil/distilled water extract. Percentage MC, total C, N and P were analysed using oven dried soil (105 °C to constant weight). C and N content was determined using a Flash 2000 organic elemental analyser (Thermo Scientific, CE Instruments Ltd, Wigan, UK) and P was determined colorimetrically according to Saunders and Williams (1955) on a FLUOStar Omega microplate reader (BMG Labtech, GmbH, Germany). $P_{organic}$ was calculated by subtracting inorganic P ($P_{inorganic}$) from total P (P_{total}), extracted using 0.5 M sulphuric acid digest for 16 h, with P_{total} digested after a 4 h ignition at 550 °C.

Soil solution was extracted according to the centrifugal-drainage procedure of Giesler and Lundström (1993). Briefly, soil in a 1:1 (*v/v*) soil/distilled water was centrifuged after gentle mixing for 30 s (4000 g, 15 min, 20 °C) to obtain water extractable soil solution and the collected solutions were frozen at −20 °C prior to analysis. Soil solution samples were analysed according to Boddy et al. (2007) for DOC and total dissolved N (TDN) using a Shimadzu TOC-V-TN analyser (Shimadzu Corp.). Nitrate (NO_3^-) was determined colorimetrically by the Cu-Zn-hydrazine reduction method of Downes (1978) and ammonium (NH_4^+) by the salicylate-hypochlorite procedure of Mulvaney (1996); dissolved organic N (DON) was estimated by the subtraction of NO_3^- and NH_4^+ from TDN. Glucose was determined spectrophotometrically with a Glucose (GO) Assay® kit (Sigma-Aldrich, MI, USA) and water extractable-Phosphate (P_{water}) colorimetrically using the molybdate-ascorbic acid method of Murphy and Riley (1962).

2.4. Microbial activity

To enable an initial investigation into the behaviour of the microbial activity in these mineral soil floodplain systems incubations were undertaken under aerobic laboratory conditions using field-moist soils. Basal respiration was measured using an automated multi-channel infra-red gas analyser (IRGA, PP-Systems Ltd., Hitchin, UK) after a 10 h incubation at 10 °C, to reduce the impact of sub sampling on the microorganisms. SMB-C content was determined by chloroform-fumigation-extraction on 5 g of soil (24 h); soils were then extracted using 1:5 (*w/v*) ratio of 0.5 M potassium sulphate and dispersed on a reciprocal shaker for 1 h prior to being centrifuged (4000 g, 15 min, 20 °C). The solutions were filtered through Whatman 42 filters before being frozen at −20 °C for DOC analysis using a Shimadzu TOC-V-TN analyser (Shimadzu Corp., Kyoto, Japan).

Substrate mineralisation was measured using a trace amount of ^{14}C-labelled glucose according to Boddy et al. (2007). Glucose is a simple sugar common to DOC of most soils that demonstrates functional redundancy because it can be utilised by a large number of different microorganisms (Marschner and Kalbitz, 2003; Dungait et al., 2011). Briefly, 35 g of pre-incubated (24 h, 10 °C) sieved soil from each depth was placed in a sealed 50 ml polypropylene container and 0.5 ml of 0.5 mM, 1 kBq, ^{14}C-U-glucose was injected onto the soil surface of each sample (18 µg glucose-C; approximately 1% of the average soil solution glucose concentration of 38.5 µM; Amersham Biosciences UK Ltd, Chalfont St. Giles, UK). 1 ml of 2 M sodium hydroxide (NaOH) in a 1.5 ml microfuge tube was placed in the container to absorb any $^{14}CO_2$ produced, with the microfuge replaced at 0.5, 1, 2, 4, 7, 11, 22, 34, 50, 95, 171, 272, 363 and 696 h to enable $^{14}CO_2$ production to be evaluated over 29 days. The $^{14}CO_2$ in the 2 M NaOH traps was determined by liquid scintillation counting using a Wallac 1404 scintillation counter (Wallac EG&G, Milton Keynes, UK) and Optiphase 3® alkali-compatible scintillation fluid (Wallac EG&G).

2.5. Statistical and data analysis

Statistical procedures were undertaken using the software package SPSS v24 for Windows (SPSS Inc., Chicago, IL) and Microsoft Excel, with $P < 0.05$ used as the upper limit for statistical confidence. Error is reported for average data with ± standard error of the mean (SEM). Changes over depth for the background soil properties were analysed using Univariate GLM, with depth as a fixed factor. To enable direct comparison between soil solution data and bulk soil analysis, soil solution concentrations were converted from mg l^{-1} to mg g^{-1} (mg l^{-1} data: Table S1). The effect of soil and soil solution chemical properties on microbial activity were analysed using stepwise multiple linear regression (MLR). In the MLR analysis, the primary r^2 value denotes the bulk soil or soil solution property accounting for the majority of the variation in microbial activity, with each subsequent r^2 value denoting the improvement of the model fit with the additional soil property variable. Soil and soil solution parameters adding less than 5% increase in fit were excluded from the analysis. Data from both sites were amalgamated to provide an average for microbial activity for this lowland section of the river Culm.

Mineralisation data were analysed using Univariate GLM, with depth as a fixed factor, to evaluate changes in microbial metabolism of glucose over depth. In the short term (< 48 h), glucose mineralisation in soil is typically biphasic (Boddy et al., 2007). However, long-term incubations typically exhibit a triphasic pattern (Glanville et al., 2016). In agreement with this, a triphasic equation best fitted our experimental data ($r^2 = 0.99$), where substrate mineralisation was described by triple first order decay equation:

$$S = [a_1 \times \exp(-k_1 t)] + [a_2 \times \exp(-k_2 t)] + [a_3 \times \exp(-k_3 t)] \quad (1)$$

Where S is the total ^{14}C-label remaining in the soil, k_1 is the exponential coefficient describing the primary mineralisation phase – the first rapid phase of rapid $^{14}CO_2$ production is attributable to the immediate use of the substrate in catabolic processes (i.e. respiration) and approximate to the depletion rate from the soil; k_2 is the exponential coefficient describing the second, slower mineralisation phase of $^{14}CO_2$ production (possibly attributable to the subsequent turnover of ^{14}C immobilised within storage pools in the soil microbial community); and k_3 the third and slowest phase (also attributable to the turnover of ^{14}C immobilised within the soil microbial community; necromass turnover; Glanville et al., 2016). The parameters a_1, a_2, and a_3 describe the size of pools associated with exponential coefficients k_1, k_2 and k_3, and t is time. The half-life of C within pool a_1 can be estimated using the equation:

$$t_{½} = \ln(2) / k_1 \quad (2)$$

(Paul and Clark, 1996). As discussed in Glanville et al. (2016), we do not know enough about the connectivity between pools a_1, a_2 and a_3 so we are unable to calculate with certainty the half time for pool a_2 and a_3. It is unlikely that the three pools are discrete and there are likely to be interactions between the pools; although the triphasic model is a very good fit to the data, biological significance cannot be assumed. Turnover times of individual organisms for the processes represented in pool a_1 (catabolic energy production) may overlap into pool a_2 (storage) for different organisms, which could affect parameter estimates for the size and turnover of separate pools. It is possible that the turnover of pools a_2 and a_3 would have to metabolise through pool a_1 during turnover. Pool a_1 is functionally distinct in that it is the rapid use of substrate for energy production, but there is large uncertainty for pools a_2 and a_3. To enable an estimation of the C use efficiency, the amount of substrate immobilised or sequestered in the soil can be calculated from the amount of ^{14}C immobilised relative to the total ^{14}C added via the equation (Jones et al., 2012):

$$^{14}\text{C use} = a_2 + a_3 / (a_1 + a_2 + a_3) \quad (3)$$

Table 1
Selected soil and soil solution properties over depth. Values represent means ± SEM ($n > 6$). The symbols * and *NS* (not significant) indicate the significant differences at the $P < 0.05$ level over depth, with superscript letters denoting the significant differences between depths.

Soil property	Sample depth (m)						*Sig. Diff.*
	0.0–0.2 ($n = 12$)	0.2–0.7 ($n = 12$)	1.0–1.5 ($n = 10$)	1.5–2.0 ($n = 10$)	2.0–2.5 ($n = 6$)	2.5–3.0 ($n = 6$)	
Silt (%)	67.84 ± 2.72^{a}	68.63 ± 2.05^{a}	56.69 ± 3.50^{a,b,c}	52.82 ± 1.90^{b,c}	47.22 ± 4.46^{c}	60.27 ± 1.98^{a,b}	*
Clay (%)	15.48 ± 1.08^{a}	16.15 ± 0.80^{a}	12.53 ± 1.01^{a,b}	12.71 ± 1.05^{a,b}	9.46 ± 0.90^{b}	13.26 ± 1.36^{a,b}	*
Moisture content (%)	32.77 ± 1.17^{a}	22.51 ± 0.94^{b}	21.40 ± 0.88^{b}	15.19 ± 0.80^{c,d}	18.32 ± 2.89^{b,c}	12.70 ± 0.60^{d}	*
pH	5.06 ± 0.11	5.12 ± 0.12	4.64 ± 0.17	5.29 ± 0.37	5.50 ± 0.57	5.67 ± 0.36	*NS*
Total C (g kg^{-1})	41.36 ± 2.79^{a}	16.59 ± 1.56^{b}	2.97 ± 0.35^{c}	2.32 ± 0.46^{c}	2.85 ± 1.27^{c}	1.23 ± 0.25^{c}	*
Total N (g kg^{-1})	4.27 ± 0.30^{a}	1.86 ± 0.16^{b}	0.39 ± 0.03^{c}	0.31 ± 0.04^{c}	0.36 ± 0.07^{c}	0.29 ± 0.02^{c}	*
Total P (g kg^{-1})	1.05 ± 0.11^{a}	0.44 ± 0.04^{b}	0.23 ± 0.02^{b}	0.20 ± 0.03^{b}	0.21 ± 0.02^{b}	0.25 ± 0.02^{b}	
Org. P (g kg^{-1})	0.69 ± 0.08^{a}	0.30 ± 0.03^{b}	0.05 ± 0.02^{c}	0.06 ± 0.02^{c}	0.02 ± 0.01^{c}	0.05 ± 0.02^{c}	*
DOC (mg C g^{-1})	15.25 ± 1.83^{a}	10.73 ± 2.08^{a,b}	4.29 ± 0.69^{b,c}	2.87 ± 0.37^{c}	3.43 ± 1.02^{c}	2.67 ± 0.94^{c}	*
DON (mg N g^{-1})	4.17 ± 0.62^{a}	2.35 ± 0.45^{b}	0.24 ± 0.12^{c}	0.16 ± 0.07^{c}	0.17 ± 0.11^{c}	0.22 ± 0.19^{c}	*
Glucose (mg C g^{-1})	0.75 ± 0.10	0.51 ± 0.08	0.75 ± 0.15	0.62 ± 0.33	0.51 ± 0.17	0.19 ± 0.05	*NS*
PO_4 (mg P g^{-1})	0.26 ± 0.01^{a}	0.18 ± 0.01^{b}	0.15 ± 0.01^{b,c}	0.11 ± 0.01^{c,d}	0.13 ± 0.02^{c,d}	0.10 ± 0.01^{d}	*
NO_3^- (mg N g^{-1})	12.61 ± 0.96^{a}	5.18 ± 0.99^{b}	0.28 ± 0.01^{c}	0.21 ± 0.02^{c}	0.38 ± 0.07^{c}	0.37 ± 0.10^{c}	*
NH_4^+ (mg N g^{-1})	0.19 ± 0.01	0.20 ± 0.07	0.13 ± 0.01	0.13 ± 0.02	0.14 ± 0.05	0.09 ± 0.02	*NS*

3. Results

3.1. Variation in soil properties at different depths in the soil profile

Soil total C and N content declined exponentially with increasing depth. All deep subsoil samples (> 1.0 m) were statistically similar to each other, but topsoil, subsoil and deep subsoil were significantly different (Table 1; $r^2 = 0.86$ for both C and N content, Fig. S2). Total C had an 18-fold reduction from topsoil to the average deep subsoil (41.4 ± 2.8 g C kg^{-1} at 0–0.2 m to 2.4 ± 0.3 g C kg^{-1} at 1.0–3.0 m), and total N a 13-fold reduction (0.0–0.2 m: 4.3 ± 0.3 g N kg^{-1} to 1.0–3.0 m: 0.3 ± 0.02 g N kg^{-1}). In accordance with Kemmitt et al. (2008b), total N was linearly correlated to total C ($r^2 = 0.99$). Particle size analyses of silt and clay also were significantly different over depth ($P < 0.05$, Table 1), with a weak linear decline over depth ($r^2 = 0.28$ for silt and $r^2 = 0.20$ for clay, Fig. S2). pH did not vary significantly, with an average pH of 5.1 ± 0.1. P_{total} and $P_{organic}$ also declined exponentially with depth (Table 1) with P_{total} declining from 1.1 ± 0.1 to 0.25 ± 0.02 g P kg^{-1} ($r^2 = 0.70$; Fig. S2); and $P_{organic}$ from 0.7 ± 0.1 to 0.1 ± 0.02 g P kg^{-1} ($r^2 = 0.75$, Fig. S2).

There was a significant linear correlation between total C compared to P_{total} and calculated $P_{organic}$, with a similar correlation observed for N in these riparian soils (Table 1; $r^2 = > 0.80$ for N and C, Fig. S3). Ratios of C:N, C:P_{total} and N:P_{total} linearly declined with increasing depth (Table 2; $r^2 = 0.34$–0.44, Fig. S2). C and N had a weak linear response to $P_{inorganic}$ ($r^2 = < 0.15$, Fig. S4). The intercept of the linear regression to total C of 0.152 was comparable to the average $P_{inorganic}$ content below 0.2 m (Fig. S3; 0.17 ± 0.02 g P kg^{-1} and median value for soils < 0.2 m = 0.16). This indicates a consistent background level of $P_{inorganic}$ from the soil parent material, with additional $P_{inorganic}$ in the topsoil. Ratios of C:$P_{organic}$ and N:$P_{organic}$ demonstrated no statistically significant variation over depth (C:$P_{organic}$ median value: 53.6 and N:$P_{organic}$ median value: 6.6). The reciprocal value of the gradient of C vs. $P_{organic}$ (63.7) and N vs. $P_{organic}$ (6.8) both gave similar values to the median ratios for C:$P_{organic}$ and N:$P_{organic}$. The outlying data points containing low $P_{organic}$ are both from cores in recent cut-offs, which contained greater sand concentrations, and therefore could be an artefact of deposition (Fig. S3).

DOC and DON concentrations in soil solution decreased exponentially with increasing depth, following a similar pattern to total C and N. Deep subsoil (1.0–3.0 m) samples were found to have no significant difference from each other, but were significantly different from topsoil and subsoil samples (Table 1; DOC: $r^2 = 0.53$, DON: $r^2 = 0.63$; Fig. S2). However, the rate of decline of DOC was less than for total C, having a 5-fold reduction in DOC (0.0–0.2 m: 15.3 ± 0.3 mg C g^{-1} to 1.0–3.0 m: 3.4 ± 0.4 mg C g^{-1}). DON was linearly correlated to DOC ($r^2 = 0.79$). DOC demonstrated linear correlations to total C ($r^2 = 0.51$; Fig. S4), SMB ($r^2 = 0.50$; Fig. S4), basal respiration ($r^2 = 0.96$; Fig. S4) and NO_3^- ($r^2 = 0.32$; Fig. S4). NO_3^- and P_{water} also declined exponentially over depth, with very low NO_3^- concentrations below 1 m (< 0.4 mg N g^{-1}, decreasing from 12.6 ± 1.0 mg N g^{-1} in 0–0.2 m; Table 1; NO_3^- $r^2 = 0.83$, P_{water} $r^2 = 0.71$; Fig. S2). NH_4^+ and glucose concentrations did not change significantly over depth (Table 1).

3.2. Microbial activity at different depths in the soil profile

Background measurements of soil microbial activity from basal soil respiration, metabolic quotient (qCO_2) and SMB-C content declined exponentially with depth (Fig. 2; SMB-C: from 498 ± 28 to 193 ± 20 μg C g^{-1}, $r^2 = 0.67$; respiration: from 3.3 ± 0.3 to 0.2 ± 0.03 μg CO_2 g^{-1} h^{-1}, $r^2 = 0.76$; and qCO_2 from 1.8 ± 0.2 μg CO_2-C g^{-1} (μg C_{SMB})$^{-1}$ h^{-1} to 0.3 ± 0.04 μg CO_2-C g^{-1} (μg C_{SMB})$^{-1}$ h^{-1}, $r^2 = 0.71$). Deep subsoil was significantly different from topsoil,

Table 2
Stoichiometric nutrient ratios in the riparian soil over depth. Values represent means ± SEM ($n > 6$). The symbols * and *NS* (not significant) indicate the significant differences at the $P < 0.05$ level over depth, with superscript letters denoting the significant differences between depths.

Sample depth (m)	C:N	C:P_{total}	C:$P_{inorganic}$	C:$P_{organic}$	N:P_{total}	N:$P_{inorganic}$	N:$P_{organic}$
0.0–0.2 ($n = 12$)	9.7 ± 0.1^{a}	43.7 ± 2.7^{a}	142.5 ± 16.1^{a}	71.9 ± 15.5	4.1 ± 0.5^{a}	14.7 ± 1.7^{a}	6.8 ± 1.6
0.2–0.7 ($n = 12$)	8.9 ± 0.2^{a}	39.0 ± 3.8^{a,b}	177.3 ± 23.0^{a}	68.2 ± 15.2	4.4 ± 0.5^{a}	20.5 ± 2.7^{a}	7.5 ± 1.6
1.0–1.5 ($n = 10$)	7.6 ± 0.5^{a}	15.4 ± 2.5^{c}	20.1 ± 3.9^{b}	88.8 ± 22.0	1.9 ± 0.4^{b}	2.7 ± 0.5^{b}	18.8 ± 5.7
1.5–2.0 ($n = 10$)	7.6 ± 1.0^{a,b}	17.9 ± 5.0^{c}	32.4 ± 10.3^{b}	49.7 ± 10.2	2.1 ± 0.4^{b}	3.7 ± 0.9^{b}	6.1 ± 1.0
2.0–2.5 ($n = 6$)	7.8 ± 2.0^{a,b}	19.3 ± 11.0^{b,c}	19.3 ± 11.3^{b}	74.2 ± 33.1	2.1 ± 0.7^{b}	2.1 ± 0.7^{b}	5.9 ± 2.1
2.5–3.0 ($n = 6$)	4.2 ± 0.6^{b}	5.2 ± 1.1^{c}	6.5 ± 1.5^{b}	46.5 ± 20.1	1.2 ± 0.1^{b}	1.5 ± 0.2^{b}	5.7 ± 0.9
Sig. Diff	*	*	*	*NS*	*	*	*NS*

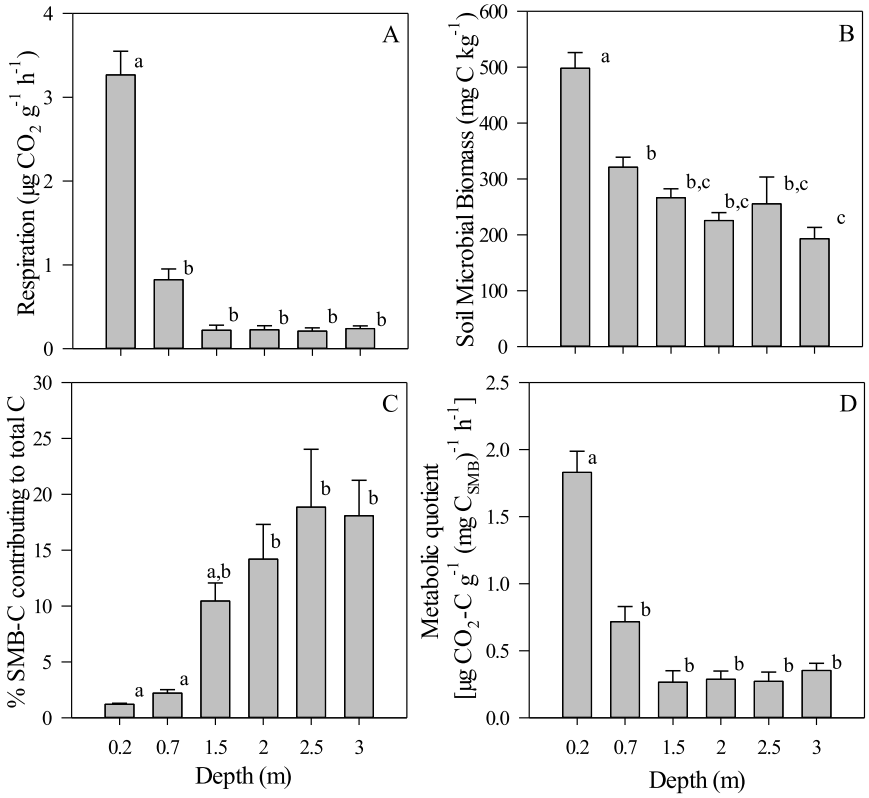

Fig. 2. Indicators of microbial activity from (a) basal respiration, (b) Soil Microbial Biomass (SMB-C) content, (c) % contribution of SMB-C to total C and (d) metabolic quotient for the lowland river Culm grassland soil over a depth of 0–3.0 m; with letters denoting the significant differences between depths (mean ± SEM; $n = 12$: 0.0–0.7 m, $n = 10$: 1.0–2.0 m, $n = 6$: 2.0–3.0 m).

with the 0.2–0.7 m subsoil being a transitionary layer between topsoil and subsoil. Basal respiration, qCO_2 and SMB-C were linearly correlated to total C ($r^2 = 0.80$, $r^2 = 0.76$, and $r^2 = 0.66$ respectively; Fig. S4) and to total N (respiration: $r^2 = 0.80$, qCO_2: $r^2 = 0.76$, and SMB-C: 0.65; Fig. S4). SMB-C also correlated linearly to basal respiration ($r^2 = 0.62$). The percentage contribution of SMB-C to total C increased exponentially with increasing depth (Fig. 2; $r^2 = 0.74$, from 1.2 ± 0.1% in the topsoil to 18.1 ± 3.2% by 2.5–3.0 m). The 15-fold reduction in basal respiration from topsoil to deep subsoil was reduced in the metabolic quotient (respiration per unit of SMB) to a 6-fold reduction in the deep subsoil.

Microbial activity was further investigated by monitoring the evolution of $^{14}CO_2$ from the soil following addition of a tracer of ^{14}C-U-glucose, which best fitted a triphasic model for $^{14}CO_2$ loss over the four-week incubation period at 10 °C (Fig. 3; Table 3). Average recovery of $^{14}CO_2$ from the soil was similar at all depths ($P > 0.05$; 81 ± 2%). Mineralisation rates for the first phase (k_1) of the triphasic metabolism of ^{14}C-U-glucose decreased exponentially with increasing depth ($r^2 = 0.55$, Fig. S5). Turnover rates of glucose in the topsoil (0.0–0.2 m) being 2.0 ± 0.1 h, subsoil (0.2–0.7 m) 4.1 ± 0.6 h; and was slowest in the deep subsoil (1.0–3.0 m, no significant difference between deep subsoil samples) at 11.4 ± 1.7 h (Table 3; $P < 0.001$). The slower phase coefficients (k_2 and k_3), attributable to the turnover of ^{14}C incorporated into the SMB (describing the metabolism of metabolites, storage compounds, extracellular enzymes and necromass turnover) behaved differently over depth (Table 3). Second phase exponential coefficients (k_2) were significantly different over depth and fitted a weak exponential decay curve, although there was greater variation in the deep subsoil (Table 3; $r^2 = 0.34$; Fig. S5). Extrapolating the rate calculation for $t_{½}$ gave an approximate residence time for k_2 of 16 h in the topsoil (0.0–0.2 m), increasing to 47 h in the deep subsoil (1.0–3.0 m). Third phase coefficient k_3 demonstrated no significant difference over depth, with a median value of 0.0012 h^{-1} (approx. 24 d).

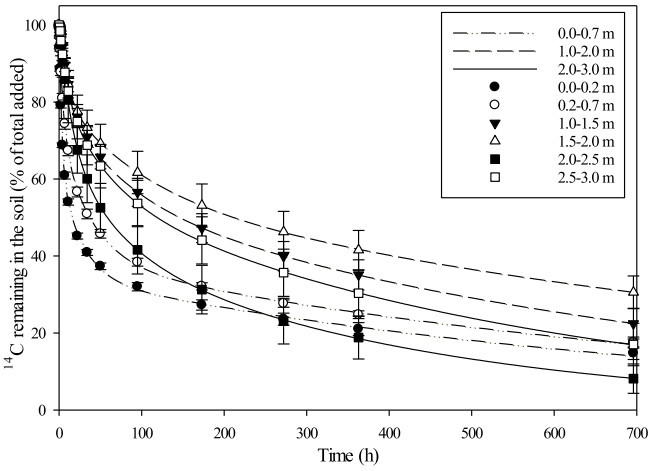

Fig. 3. Mineralisation kinetics following the addition of ^{14}C-U-glucose to riparian soil, incubated at 10 °C for four weeks. Mineralised $^{14}CO_2$ was trapped in 2 M NaOH and the percentage of added ^{14}C remaining in the soil plotted over time. Symbols are means ± SEM ($n = 12$: 0.0–0.7 m, $n = 10$: 1.0–2.0 m, $n = 6$: 2.0–3.0 m). Lines represent fits of the triple exponential decay model to the experimental data.

The pools a_1, a_2 and a_3 associated with the exponential coefficients k_1, k_2 and k_3 varied in their response over depth. The initial pool (a_1; associated with immediate catabolic use) decreased with increasing depth, with a weak exponential decay curve fitting the data (a_1: $P = 0.05$; Table 3; $r^2 = 0.20$: Fig. S5; from 0.0 to 0.2 m: 35.2 ± 1.9% to 1.0–3.0 m: 23.7 ± 2.1%). Pool a_2 demonstrated no significant difference over depth (averaging 29.6 ± 1.0%; $P > 0.05$). The final proportion of ^{14}C allocated in the triphasic model to pool a_3 increased linearly with increasing depth, with a greater proportion of ^{14}C allocated to the deep subsoil (Table 3; $P = 0.007$; $r^2 = 0.26$: Fig. S5; from

Table 3
Parameters of the triple exponential equation describing the mineralisation of ^{14}C-U-glucose in soil solution in riparian soil, where the glucose ^{14}C is partitioned into the respired C pool a_1, or the SMB pools a_2 and a_3. The half-life (t_1) of the ^{14}C-U-glucose in soil solution pool a_1 (defined as ln(2)/k_1) and the rate constants (k_2 and k_3) for the turnover of C immobilised in the SMB pools (a_2 and a_3) are given. The symbols * and *NS* (not significant) indicate the significant differences at the $P < 0.05$ level over depth, with superscript letters denoting the significant differences between depths. Values represent means ± SEM, $n > 6$.

Depth (m)	Model parameter						
	a_1 (%)	k_1 (h^{-1})	t_1 (h)	a_2 (%)	k_2 (h^{-1})	a_3 (%)	k_3 (h^{-1})
0.0–0.2 (n = 12)	35.2 ± 2.1	0.37 ± 0.03^{a}	1.9 ± 0.1^{a}	29.0 ± 1.9	0.04 ± 0.003^{a}	36.0 ± 1.4^{a}	0.0030 ± 0.0015
0.2–0.7 (n = 12)	28.6 ± 1.7	0.22 ± 0.04^{b}	4.1 ± 0.6^{a,b}	33.0 ± 1.8	0.03 ± 0.004^{a,b}	37.9 ± 1.2^{a,b}	0.0012 ± 0.0001
1.0–1.5 (n = 10)	25.3 ± 3.1	0.08 ± 0.01^{b,c}	12.2 ± 2.7^{a,b}	29.9 ± 2.2	0.01 ± 0.003^{b,c}	46.0 ± 3.9^{a,b}	0.0015 ± 0.0003
1.5–2.0 (n = 10)	24.2 ± 3.9	0.10 ± 0.02^{b,c}	11.2 ± 3.7^{a,b}	29.0 ± 3.4	0.01 ± 0.002^{c}	47.6 ± 4.5^{a,b}	0.0009 ± 0.0002
2.0–2.5 (n = 6)	21.9 ± 5.6	0.14 ± 0.05^{b,c}	13.1 ± 4.9^{a,b}	26.9 ± 3.4	0.04 ± 0.007^{a}	52.8 ± 5.7^{b}	0.0036 ± 0.0009
2.5–3.0 (n = 6)	22.1 ± 5.9	0.11 ± 0.03^{b,c}	8.7 ± 2.1^{a,b}	26.3 ± 2.0	0.01 ± 0.005^{b,c}	52.0 ± 7.2^{b}	0.0021 ± 0.0006
Sig. Diff.	*NS*	*	*	*NS*	*	*	*NS*

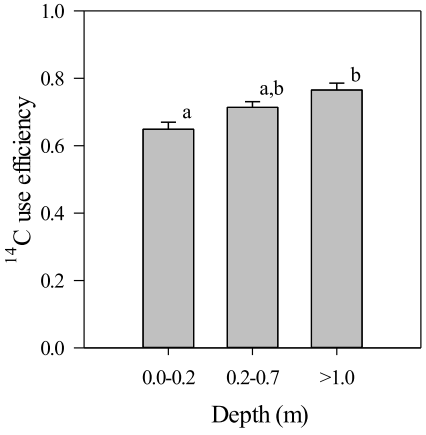

Fig. 4. Utilisation efficiency of ^{14}C labelled substrate averaged over three depths – topsoil, subsoil rooting layer and deep subsoil, values represent means ± SEM (n = 12: 0.0–0.7 m, n = 10: 1.0–2.0 m, n = 6: 2.0–3.0 m); with letters denoting the significant differences between depths.

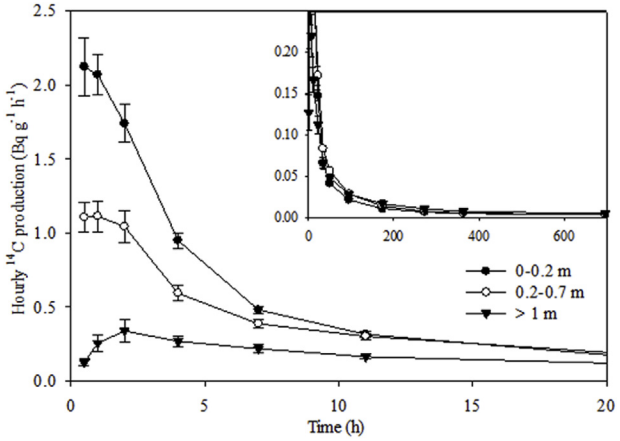

Fig. 5. Production rate of $^{14}CO_2$ following the addition of ^{14}C-U-glucose for riparian soil in the topsoil (0–0.2 m), rooting layer subsoil (0.2–0.7 m) and deep soil (> 1 m). Demonstrating the different pattern of production over time 0–20 h, with the insert of 0 h to the final sampling at 696 h. Values represent means ± SEM (n = 12: 0.0–0.7 m, n = 10: 1.0–2.0 m, n = 6: 2.0–3.0 m).

0.0 to 0.2 m: 33.0 ± 1.6% to 1.0–3.0 m: 48.9 ± 2.5%). The riparian soil varied in C use efficiency (CUE) over depth (Fig. 4), with CUE increasing with depth. However, depth was only significant when the soils were averaged over the three depths (topsoil, subsoil and deep subsoil), with a greater proportion of ^{14}C immobilised at depth (0.0–0.2 m: 0.65 ± 0.02, 0.2–0.7 m: 0.71 ± 0.02, 1.0–3.0 m: 0.77 ± 0.02; P = 0.003).

Converting the production of $^{14}CO_2$ from the riparian soils into an hourly rate per gram of soil enabled the rate of microbial response to ^{14}C-labelled substrate addition to be investigated. The initial rate of production correlated linearly to the exponential coefficient for catabolic mineralisation (k_1: Bq g^{-1} h^{-1}, r^2 = 0.72). The rate of production at the initial sampling period (0.5 h), over the 3 m soil profile, best fitted an exponential decay curve with topsoil, subsoil and deep subsoil samples being significantly different ($P < 0.001$; Fig. 5; 0.0–0.2 m: 2.12 ± 0.19, 0.2–0.7 m: 1.11 ± 0.10, 1.0–3.0 m: 0.13 ± 0.02 Bq g^{-1} h^{-1}; r^2 = 0.79, Fig. S5). Initial deep subsoil Bq g^{-1} h^{-1} production rates were 17 times smaller than the topsoil rate. However, when normalised for the quantity of SMB, the initial sampling period Bq g^{-1} h^{-1} mg^{-1} SMB-C production was only 7 times slower in the deep subsoil (0–0.2 m: 4.41 ± 0.51, 0.2–0.7 m: 3.51 ± 0.34, 1.0–3.0 m: 0.63 ± 0.13 Bq g^{-1} h^{-1} mg^{-1} SMB-C). Unlike topsoil and subsoil, deep subsoil achieved maximal Bq g^{-1} h^{-1} production at 2 h rather than at the initial 0.5 h sampling (Fig. 5), with nearly 3 times greater rates of production at 2 h (an increase from 0.13 ± 0.02 to 0.34 ± 0.08 Bq g^{-1} h^{-1}). Topsoil and subsoil production rates were statistically similar after 4 h, with significantly reduced deep subsoil (> 1.0 m) production rates ($P < 0.001$). After 22 h subsoil (0.2–0.7 m) production rates were in excess of the topsoil, however this was not significantly different until sampling at 95 h ($P < 0.03$). After 173 h the rate of production in the deep subsoil exceeded that of the topsoil and subsoil (0.0–0.7 m), although only the topsoil had significantly smaller Bq g^{-1} h^{-1} production rates ($P < 0.03$).

3.3. Influence of selected soil properties on microbial activity

Microbial activity (as measured by basal respiration; SMB; mineralisation rate constants k_1, k_2 and k_3; and rates of $^{14}CO_2$ production (Bq g^{-1} h^{-1} or Bq g^{-1} h^{-1} μg^{-1} SMB-C) was compared with the measured soil and soil solution chemical parameters (Table 1) using MLR analysis (Table 4). Over the whole profile the majority of the variation in microbial activity could be explained by the total C, N and NO_3^- concentrations in the soil (respiration – C: r^2 = 0.92; SMB-C – C: r^2 = 0.70; k_1 – NO_3^-: r^2 = 0.70; k_2 – NO_3^-: r^2 = 0.52; initial Bq g^{-1} h^{-1} – NO_3: r^2 = 0.83 and initial Bq g^{-1} h^{-1} SMB^{-1} – NO_3^-: r^2 = 0.59), with the exception of k_3 where there was no fit to the chemical properties. N:$P_{organic}$ ratios, MC and silt were secondary contributors improving the fit in the model for microbial activity. Although the overall model demonstrated no co-linearity, the individual components of C and N demonstrated co-linearity in their effect. Throughout all MLR analysis, depth had no effect on microbial activity when compared to the other chemical properties.

MLR by depth increment yielded different results for topsoil

Table 4
Multiple linear regression analysis of microbial activity versus selected soil chemical properties by depth, adjusted r^2 values, constant (slope of the regression) and Beta values (gradient of the regression). The primary r^2 value denotes the soil and soil solution property accounting for the majority of the variation in the parameter of microbial activity, with each subsequent soil property r^2 value denoting the improvement of the model fit with the additional variable. Soil and soil solution parameters adding less than 5% increase in fit were excluded from the analysis.

Parameter of microbial activity	MLR 0-3 m (n = 56)	MLR 0–0.2 m (n = 12)	MLR 0.2–0.7 (n = 12)	MLR 1-3 m (n = 32)
Respiration	C: r^2 = 0.92 Constant: −0.014 *B* C: −0.070	C: r^2 = 0.78 Constant: 0.003 *B* C: 0.073	NO_3^-: r^2 = 0.80 Constant: 0.212 *B* NO_3^-: 0.118	No fit
SMB	C: r^2 = 0.70 Constant: 222.686 *B* C: 6.432	Glucose: r^2 = 0.46 NO_3^-: r^2 = 0.66 NH_4^+: r^2 = 0.81 $C:P_{total}$: r^2 = 0.91 Constant: 871.685 *B* Glucose: 331.575 *B* NO_3^-: 7.353 *B* NH_4^+: −2611.008 *B* $C:P_{total}$: −4.897	No fit	P_{water}: r^2 = 0.41 Constant: 68.697 *B* P_{water}: 1367.938
k_1	NO_3^-: r^2 = 0.70 Constant: 0.101 *B* NO_3^-: 0.024	Clay: r^2 = 0.46 Constant: 0.114 *B* Clay: 0.017	NO_3^-: r^2 = 0.52 NH_4^+: r^2 = 0.73 Clay: r^2 = 0.82 Constant: 0.292 *B* NO_3^-: 0.050 *B* NH_4^+: −0.397 *B* Clay: −0.016	C:N: r^2 = 0.22 Constant: 0.187 *B* C:N: −0.012
k_2	NO_3^-: r^2 = 0.52 $N:P_{organic}$: r^2 = 0.59 MC: r^2 = 0.64 Constant: 0.027 *B* NO_3^-: 0.004 *B* $N:P_{total}$: 0.000 *B* MC: −0.001	Clay: r^2 = 0.54 Constant: 0.007 *B* Clay: 0.002	NO_3^-: r^2 = 0.93 Constant: 0.004 *B* NO_3^-: 0.004	$N:P_{organic}$: r^2 = 0.14 P_{water}: r^2 = 0.25 Constant: 0.002 *B* $N:P_{organic}$: 0.000 *B* P_{water}: −0.175
k_3	No fit	$C:P_{organic}$: r^2 = 0.89 NO_3^-: r^2 = 0.95 Constant: −0.012 *B* $C:P_{organic}$: 0.000 *B* NO_3^-: 0.001	$P_{inorganic}$: r^2 = 0.81 Constant: 0.001 *B* $P_{inorganic}$: 0.003	C:N: r^2 = 0.16 Clay: r^2 = 0.32 Constant: 0.006 *B* C:N: 0.000 *B* Clay: 0.000
Initial 0.5 h Bq g^{-1} h^{-1}	N: r^2 = 0.83 Constant: 0.055 *B* N: 0.471	No fit	C: r^2 = 0.77 MC: r^2 = 0.85 Constant: 0.792 *B* C: 0.067 *B* MC: −0.036	P_{water}: r^2 = 0.40 $P_{inorganic}$: r^2 = 0.63 N: r^2 = 0.72 Constant: 0.248 *B* P_{water}: −3.646 *B* $P_{inorganic}$: 0.995 *B* N: 0.487
Initial 0.5 h Bq g^{-1} h^{-1} SMB^{-1}	NO_3^-: r^2 = 0.59 Silt: r^2 = 0.66 Constant: −0.002 *B* NO_3^-: 0.000 *B* Silt: 5.063×10^{-5}	No fit	$N:P_{organic}$: r^2 = 0.71 $P_{organic}$: r^2 = 0.92 Constant: −0.001 *B* $N:P_{organic}$: 0.000 *B* $P_{organic}$: 0.007	P_{water}: r^2 = 0.41 $P_{inorganic}$: r^2 = 0.57 N: r^2 = 0.67 Constant: 0.001 *B* P_{water}: −0.022 *B* $P_{inorganic}$: 0.005 *B* N: 0.003

(0–0.2 m), subsoil (0.2–0.7 m) and deep subsoil (1.0–3.0 m; Table 4). Topsoil (0.0–0.2 m) demonstrated the greatest difference from the overall soil profile model, with no fit for initial rates of production (Bq g^{-1} h^{-1} and Bq g^{-1} h^{-1} μg^{-1} SMB-C). For k_1 and k_2, texture became a significant property (r^2 = 0.46 and 0.54 respectively). As for the overall MLR model, topsoil respiration rates were still strongly correlated to total C. In the subsoil (0.2–0.7 m) microbial activity parameters were dominated by NO_3^-, N and P content, in contrast to the importance of C in the overall model. NH_4^+, clay and MC were secondary variables, in the subsoil. However, there was no fit for SMB to the measured subsoil soil properties. Increased correlation with P and stoichiometric variables were observed in the deep subsoil (> 1.0 m) for ^{14}C mineralisation parameters and SMB. There was no fit for respiration with the measured deep subsoil properties.

4. Discussion

4.1. Deep floodplain soils support a large microbial population

We tested the hypothesis that deep floodplain soil systems support a relatively large microbial population and found that, as in Rumpel and Kögel-Knabner (2010), SMB-C declined over depth (Fig. 6). However, the decline was not as rapid as previously reported for other non-riparian soils (Federle et al., 1986; Fontaine et al., 2007). Here, the population only decreased to approximately half of the surface population. Topsoil SMB-C concentrations (498 μg g^{-1}) in the lowland floodplain of the River Culm was similar to the river bank SMB-C values of 518 μg g^{-1} in Ettema et al. (1999) and 448 μg SMB-C g^{-1} in Kirkby et al. (2013). As reported in other studies (both riparian and non-riparian), our results demonstrated a rapid decline of total C with soil depth, with 70% of total C found within the topsoil in the first metre (Bai et al., 2005; Walling et al., 2006; Torres-Sallan et al., 2017). C:N ratios also decreased with increasing depth, which is generally attributed to increasingly processed and stabilised OM pool in the deeper soil

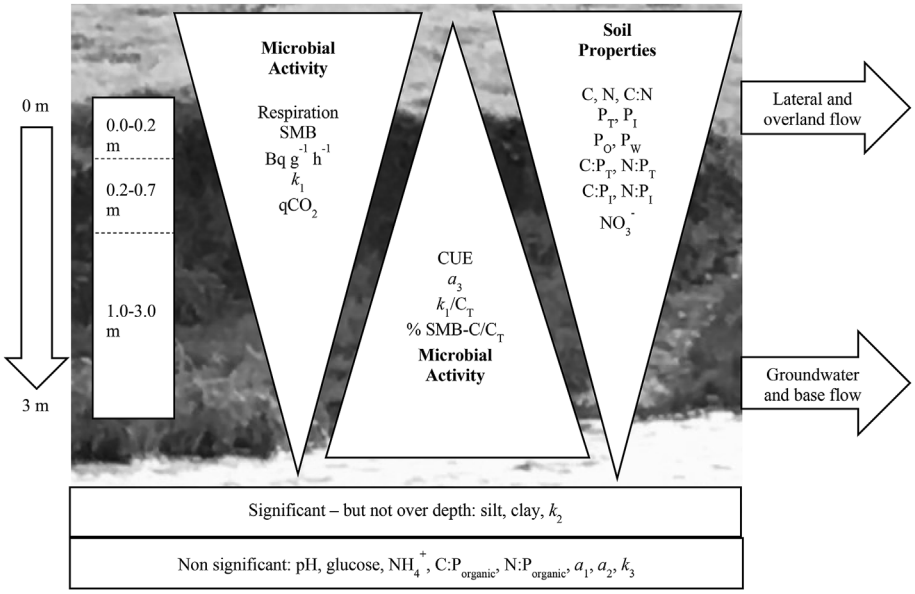

Fig. 6. The variation in soil properties and microbial response to added ^{14}C-glucose over depth, with triangles representing the reduction or increase in microbial activity and soil parameters, adapted from (Marín-Spiotta et al., 2014). With surface soils containing elevated C, N and P and having greater microbial activity as measured by respiration, microbial biomass, metabolic quotient (qCO_2) and initial $^{14}CO_2$ mineralisation rate constant k_1. Whereas deep subsoil demonstrated higher CUE and a greater proportion of total C consisting of SMB-C, with initial mineralisation for k_1 normalized by total C also having greater values in the deep subsoil compared to the topsoil and rooting zone subsoil. Non significant variables and variables demonstrating significant differences that were not related to increasing depth are shown below.

profile (Rumpel and Kögel-Knabner, 2010; Salomé et al., 2010; Kirkby et al., 2013; Gregory et al., 2016; Wordell-Dietrich et al., 2017).

The proportion of total C as SMB-C increased over depth from 1.2% in the topsoil to 14.6% in the deep subsoil (1.0–3.0 m; Fig. 6), which is substantially greater than the reported microbial quotient range of 0.3–7.0% of SOC (von Lützow et al., 2007; Brookes et al., 2008; Zehetner et al., 2009; Gonzalez-Quiñones et al., 2011). Chaopricha and Marín-Spiotta (2014) also reported an increasing microbial proportion of deep soil C as a consequence of soil burial occurring under a range of circumstances, e.g., erosion in sloping lands. This is in contrast to the analysis of arable soil profiles at Rothamsted by Jenkinson et al. (2008) where the proportion of SOC as SMB decreased with depth. Kramer et al. (2013) linked declining SMB populations over depth with decreased substrate quality. This may be less significant in floodplain soils where, even though the total C content declined to 6% of surface concentration, the regular flushing of recent DOC may enable the survival of the large proportion of SMB in the subsoil, or may flush topsoil SMB through the soil profile. DOC was measured at all depths in these floodplain soils, with an increased proportion of total C as DOC with increasing depth, and not predominantly in the topsoil as reported in Qualls and Haines (1992) and von Lützow et al. (2007). However, it cannot be ruled out that the presentation of DOC at all depths in this study may be an artefact of the extremely high levels of rainfall in SW England in 2008 driving increased flushing of DOC through the soil profile (Fig. 1; Met Office, 2017).

The DOC concentrations in the deep subsoil were comparable to that measured in lateral subsurface flow during winter in a managed grassland in SW England, reported by Sandford et al. (2013; 5–23 mg C l^{-1}). They proposed that the increased proportion of total C as DOC was due to the release of previously stabilised SOC or as novel inputs from leaching or sublateral flow. Wordell-Dietrich et al. (2017) determined that a greater proportion of the subsoil C was labile by measuring relative rates of mineralisation in soil from different depths. The SMB is often considered to be the main component of the active SOC pool in models of soil C dynamics and therefore an increase in labile C at depth may be coincident with an increased proportion of SMB (von Lützow et al., 2007). Furthermore, von Lützow et al. (2007) note that whilst labile C is often described as bioavailable, several studies describe the poor degradability of up to 40% DOC extracted from soils. Similarly, Jones et al. (2018) suggest that subsoil DOC accumulation is predominantly highly processed, more recalcitrant DOC, recognised by relatively increased DOC:DON ratios in an arable subsoil. Keller and Bridgham (2007) indicate that aerobic conditions in wetlands can result in a rapid loss of labile C, resulting in reduced substrate quality. DOC can also accumulate under anaerobic conditions where iron reduction has occurred in mineral soils, releasing C held in iron oxide complexes (Huang and Hall, 2017), which could be a factor in these deep subsoils during redox oscillations.

4.2. Contrasting microbial response to DOC over depth

We tested the second part of our hypotheses, i.e., that the relatively large SMB was metabolically alert and able to respond rapidly to substrate supply, by measuring basal respiration and the mineralisation of a trace amount of ^{14}C-glucose as a proxy for microbial activity in these deep floodplain soils. Nearly all (95%) of the total respiration of the floodplain soil occurred in the 0–0.7 m depth with a 15-fold reduction in respiration rates in the deep subsoil (similar to Jenkinson and Coleman, 2008). However, estimated microbial activity as qCO_2 was 7 times smaller in the deep subsoil. Microbial activity declined more rapidly than SMB concentration that indicated a 50% smaller microbial community size in deep soils compared to top soils, which is comparable to the observations of phosphoplipid fatty acid (PLFA) abundance by Federle et al. (1986). Wordell-Dietrich et al. (2017) also reported, when basal respiration was normalised to total C (rather than mass of soil), respiration rates that were three times greater in the deep subsoil than the topsoil. Salomé et al. (2010) reported no signficant difference in respiration rates of soils from different depth horizons of an arable soil up to 1.0 m depth. These reports are contrary to the general theory of reduced microbial activity with depth in soils, suggesting that the controls on C mineralisation in deep soils are more complex than merely the size of the microbial population as a predictor of activity. Therefore, in hydrologically dynamic floodplain soils where regular inputs of up to 70 mg l^{-1} DOC can occur, the long term activity of a smaller but highly responsive SMB may be preserved (Valett et al., 2005; Zehetner et al., 2009).

To further test our hypotheses, we utilised a ^{14}C-labelled labile tracer (i.e., glucose) as a proxy for the potential turnover rates for DOC over depth in floodplain soils under aerobic conditions. The amount of glucose added was less than 1% of the average measured glucose concentration of the floodplain soils considered in this study, and as such was deemed not to be sufficient to be considered as a substrate amendment as the addition was well within natural concentrations (with glucose concentration having no significant difference over depth). This amount of C is also unlikely to stimulate microbial growth, thereby providing a more realistic estimate of microbial C use and

partitioning. In addition, the glucose addition of 0.25 μM was less than the reported concentrations of carbohydrates in stream DOC (i.e., 0.42–12.4 μM; Gremm and Kaplan, 1998). However, unlike glucose, SMB, DOC and total C decreased over depth and therefore the ratio of glucose addition proportionally increased over depth compared to SMB, DOC and total C content. However, each variable increased at a different rate (2-fold increase in glucose:SMB from topsoil to deep subsoil, 5-fold glucose:DOC, 28-fold glucose:total C). For this study we utilised a constant trace amount of glucose, but the implications of these changing ratios is an area that warrants further study to investigate the impact of the proportional increase of ^{14}C-glucose at depth.

The SMB was highly responsive to the addition of ^{14}C-glucose at all depths, as described by Kemmitt et al. (2008a) and Jones et al. (2018). The rates of turnover for the topsoil (0.0–0.2 m; $t_{½}$ 2.0 ± 0.1 h) and subsoil (0.2–0.7 m; $t_{½}$ 4.1 h) were similar to previous grassland soil mineralisation experiments, where turnover times of 0.4–5.0 h for the initial catabolic respiration of added ^{14}C-glucose were reported (Jones et al., 2005; Boddy et al., 2007; Glanville et al., 2016). Jones et al. (2005) also observed slower mineralisation rates for ^{14}C-labelled amino acids (14 h) in a non-riparian soil compared to glucose (11.4 h) in the deep floodplain subsoils of this study. While the size of the SMB-C as a proportion of total C indicated a relatively substantial soil microbial population at depth, its slower response to glucose addition suggests that it was limited by other factors, e.g., nutrient supply (Sanaullah et al., 2016). Although, when the first phase mineralisation rate constant k_1 was normalised for SMB there was no significant difference in first phase mineralisation between the soil depths. However, as with basal respiration, when k_1 was expressed per unit of C content, rate constants were faster in the deep subsoil than topsoil (comparable to Heitkötter et al., 2017 and Wordell-Dietrich et al., 2017), and in these deep floodplain subsoils the rate constants were 10 times faster. However, we recognised that proportionally more ^{14}C-glucose was available to the SMB in the deep subsoil than the shallower soil depths, and this should be accommodated as a factor in future studies. Nonetheless, our study demonstrates that there are active microbial communities up to 3 m in floodplain soils which are capable of rapidly mineralising simple sugars, like glucose, that are universally ubiquitous in soil profiles.

Mineralisation dynamics of the ^{14}C-glucose in the deep floodplain subsoil (1.0–3.0 m) were different compared to the topsoil and subsoil (0.2–0.7 m), with an observed lag time of 2 h to reach maximum mineralisation rates. Spatial separation from the added substrate due to the 50% reduction in population size in the deep subsoil makes it less likely for microorganisms to encounter added substrates (Dungait et al., 2012; Sanaullah et al., 2016). However, the 2 h lag time was faster than the previously reported 4 d lag period for deep (130–160 cm) but non-riparian subsoil after the addition of a more complex substrate (^{13}C-labelled root litter; Wordell-Dietrich et al., 2017), and very rapid compared with the 2–3 week lag time reported after addition of glucose to deep buried soil from a burial mound (Chaopricha and Marín-Spiotta, 2014). The relatively short lag period suggests that the SMB in floodplain soils up to 3 m depth are adapted and able to respond rapidly to episodic inputs of DOC from vertical or lateral flushing. Sixty-four to 86% of the DOC pulse during soil inundation in floodplains originates from the upper layers of riparian soils (Morel et al., 2009), supplying a source of substrate that is likely to be of better quality, i.e. richer in organic nutrients, than in non-riparian deep soils. The fast turnover times and shorter lag periods in deep floodplain soils suggests that the SMB are predominantly "metabolically alert" *r* strategists rather than dormant *K* strategists, e.g., spore formers, as a survival strategy to compete favourably for episodic resource supply (Hoyle and Murphy, 2007; Hoyle et al., 2008; Dungait et al., 2011, 2013). As labile C mineralisation occurs in both aerobic and anaerobic systems, with labile C often a preferential C substrate in anaerobic systems as well as aerobic, it is possible that a distinct microbial population may develop in subsurface horizons (Chaopricha and Marín-Spiotta, 2014; Keller and Wade, 2018).

We observed that more ^{14}C was allocated to microbial storage in the subsoil (pool a_3: 49% in deep subsoil compared to 36% in topsoil; Fig. 6) than to respiration (pool a_1: 24% of deep subsoil and 35% in topsoil). Furthermore, 19% of the ^{14}C label was unrecovered, and was most likely incorporated into the microbial biomass and synthesised into exuded microbial products, e.g., extracellular enzymes, and/or adsorbed onto soil minerals. In C-limited soils characteristic of deeper soils horizons, more C may be apportioned to synthesis (anabolism) and storage by microorganisms, whereas abundant C is predominantly mineralised (catabolism) in C-rich top soils (Raymond and Bauer, 2001; Hoyle et al., 2008). The former is likely the case in the relatively nutrient poor deep subsoil, where microorganisms are more efficient at assimilating available substrate, detected as an increase of CUE as C:N decreases (Sinsabaugh et al., 2013). This is in contrast to Wordell-Dietrich et al. (2017) who determined reduced CUE in subsoils. We recognise that in our experiment, the same trace amount of ^{14}C-glucose was provided to the 50% smaller microbial population in the deep subsoil (based on SMB-C concentrations) as to the topsoil, which may be reflected in the observed increase in CUE at depth.

4.3. Microbial nutrient limitation in the floodplain soil profile

The majority of soil properties declined significantly over depth and could be assigned into three depths with different characteristics: topsoil (0.0–0.2 m), subsoil (0.2–0.7 m), and deep subsoil (1.0–3.0 m). (pH did not vary over depth and it is unlikely that these soils were constrained by acidity; Jones et al., 2018). Topsoil was characterised by elevated concentrations of C, N, P, DOC and DON. The subsoil (0.2–0.7 m) acted as a transitionary layer where deeper roots and root exudates delivered fresh C (Kramer et al., 2013; Chaopricha and Marín-Spiotta, 2014). The poor C content at depth may have been exacerbated by the relatively increased microbial activity due to real priming when supplies of biologically available C were abundant (Dungait et al., 2013), and may also drive the potential for anaerobic conditions to emerge due to increased biological oxygen demand when supply outpaces gas diffusion in these deep subsoils (Keiluweit et al., 2018).

Hill et al. (2014) and Ng et al. (2014) discussed the importance of ecological stoichiometry of C:N:P in regulating microbial activity; and in these riparian soils the relationship of these three essential elements varied over depth (Fig. 6). Microbial activity in the deep subsoil was correlated with stoichiometry and P availability, whereas the overall profile MLR model was dependent on C, N and NO_3^- concentrations. According to stoichiometric decomposition theory, maximal decomposition rates occur when C, N and P match microbial requirements (Heitkötter et al., 2017). This condition was observed in the nutrient rich topsoil and, here, textural variation exerted significant control on variation on microbial activity (rate coefficients k_1 and k_2). Overall, the stoichiometry in these floodplain soils (median C:N:$P_{organic}$ of 54:7:1) compared to reported values for SMB (60:7:1; Cleveland and Liptzin, 2007; Sinsabaugh et al., 2013), indicated that a large proportion of the SOC was derived from microbial detritus (Tipping et al., 2016). However, the deep subsoil C:N ratio was below the microbial tissue quotient range of 7.3–8.6 reported in Sandford et al. (2013), and the N:P_{total} values are less than the recorded N:P of the SMB of 6.9 reported in Cleveland and Liptzin (2007), suggesting the deep soils were nutrient limited. Consequently, additions of biologically available DOC during flood events to nutrient-poor deep floodplain soils may result in the loss of SOC as stabilised SOM is mined for limiting nutrients (Craine et al., 2007; Ng et al., 2014; Heitkötter et al., 2017).

In this study, total N, DON and NO_3^- all declined exponentially, indicating potential N limitation with increasing depth (Bai et al., 2005; Jones et al., 2018, Fig. 6). N limitation has been proposed to result in a poor C sink with C metabolised for catabolic processes rather than growth (Kirkby et al., 2013). Although NH_4^+ concentrations remained unchanged over the soil profile, as in Jenkinson et al. (2008) the proportion of the soil N held as NH_4^+ increased over depth, with an 8-fold

increase. However, the same was not true for NO_3^-, where the proportion of total N held as NO_3^- declined 3-fold. The low levels of NO_3^- and proportional increase in NH_4^+ could indicate fluctuating aerobic conditions with denitrification occurring during anaerobic decomposition, with NO_3^- changed to NH_4^+ through anaerobic dissimilatory reduction, although the low available C concentrations may also limit these reactions (Keller and Bridgham, 2007; Ding et al., 2017).

The rapid response to ^{14}C-glucose without the addition of N or P also supports the suggestion that microbial activity in these subsoils are limited by access to biologically available C (Rumpel and Kögel-Knabner, 2010; Jones et al., 2018). This is also consistent with the decrease in C:N in the deep subsoil and the importance of C in the overall MLR model for respiration and SMB. Nevertheless, it is important to note that this study was undertaken using aerobic laboratory conditions and therefore, it is important to consider this constraint when interpreting a deep profile subject to episodic inundation. It is acknowledged that further work should be undertaken to ascertain microbial activity under different redox conditions due to the changes in oxygen availability, e.g., during episodes of prolonged waterlogging common in floodplains. Although glucose added to peat and paddy field soils under anaerobic conditions can be rapidly mineralised (Wang et al., 2015; Keller and Wade, 2018), it is likely that the C, N and P limitations observed in these aerobic conditions of our experiment would also be rate limiting in anaerobic systems (Hill et al., 2014). Therefore, notwithstanding the limitations of the approach, we consider these mineral floodplain soils to show evidence of a versatile microbial community capable of adapting to aerobic and anaerobic conditions due to their potential to respond rapidly to substrate availability. With these data providing an important indicator of enhanced microbial activity in an environment often thought of as a sink for C due to the rapid accumulating nature of the floodplain and low microbial activity expected at depth.

4.4. Conclusions

In accordance with our hypothesis we found a proportionally large and active SMB in the deep subsoil of these floodplain soils. Fifteen per cent of the total C measured in the deep subsoil was in the SMB, exceeding the 1% usually typically reported for topsoils. The deep floodplain soils supported a large microbial population with only a 50% reduction in SMB compared to a 94% reduction in total C. This could be a consequence of the regular flushing of DOC through the soil profile during inundation events and hyporheic flow or from the translocation of SMB during flood events. We observed an active microbial population at all depths, however, the top soil and subsoil depths (0.0–0.7 m) had a contrasting mineralisation response to the addition of labile C (^{14}C-glucose) compared to the deep subsoil (1.0–3.0 m), where a 2-h lag for maximal production of $^{14}CO_2$ was observed. This relatively short lag time indicates that the SMB in the deep subsoil remained metabolically alert to take advantage of episodic events of DOC abundance, but were restricted in their response by the likelihood of encountering substrate by a spatially dispersed and smaller microbial population. A greater proportion of the added ^{14}C-glucose was calculated to have been incorporated into the SMB in the deeper soil, with the turnover of C in pool α_3 approximating 24 d, indicating that there is the potential for labile C preservation within the SMB in deep floodplain soils. Although first phase mineralisation (k_1) decreased with increasing depth, when normalised for the SMB content in the soil there was no significant difference between the soil depths. This indicates that microbial activity in the subsoil was limited by access to biologically available C and was capable of rapid mineralisation rates when conditions allowed access to supply. However, our hypothesis requires further testing under different redox conditions and would benefit from identification of the microbial communities involved in the mineralisation of C in these systems to enable better understanding of the biological controls on C cycling in floodplain systems.

Data Access Statement

Data supporting this study are stored by the corresponding author at the University of Exeter.

Acknowledgements

This work was funded by the UK Natural Environment Research Council as part of the Impacts of Climate Change on Erosion, Sediment Transport and Soil Carbon in the UK and Europe project (NE/E011713/1). We thank Richard Jones and Neville England for assistance with the Geoprobe work; Stephen Haley and the technician team for their assistance with laboratory analysis at Exeter University; and Paul Hill, Jonathan Roberts and Gordon Turner for their assistance with laboratory analyses at Bangor University. We thank Emilie Grand-Clement for her helpful comments on the manuscript, and Sophie Green and Andrew Meade for their statistical assistance. This work represents part of the BBSRC-funded programme 'Soil to Nutrition' (BB/P01268X/1) at Rothamsted Research.

Appendix A. Supplementary data

Supplementary data related to this article can be found at http://dx.doi.org/10.1016/j.soilbio.2018.04.001.

References

Bai, J., Ouyang, H., Deng, W., Zhu, Y., Zhang, X., Wang, Q., 2005. Spatial distribution characteristics of organic matter and total nitrogen of marsh soils in river marginal wetlands. Geoderma 124, 181–192.
Beniston, J.W., Shipitalo, M.J., Lal, R., Dayton, E.A., Hopkins, D.W., Jones, F., Joynes, A., Dungait, J.A.J., 2015. Carbon and macronutrient losses during accelerated erosion under different tillage and residue management. European Journal of Soil Science 66, 218–225.
Boddy, E., Hill, P., Farrar, J., Jones, D., 2007. Fast turnover of low molecular weight components of the dissolved organic carbon pool of temperate grassland field soils. Soil Biology and Biochemistry 39, 827–835.
Bräuer, T., Grootes, P.M., Nadeau, M.-J., 2013. Origin of subsoil carbon in a Chinese paddy soil chronosequence. Radiocarbon 55, 1058–1070.
Brookes, P., Cayuela, M., Contin, M., De Nobili, M., Kemmitt, S., Mondini, C., 2008. The mineralisation of fresh and humified soil organic matter by the soil microbial biomass. Waste Management 28, 716–722.
Bullinger-Weber, G., Le Bayon, R.C., Thébault, A., Schlaepfer, R., Guenat, C., 2014. Carbon storage and soil organic matter stabilisation in near-natural, restored and embanked Swiss floodplains. Geoderma 228–229, 122–131.
Chaopricha, N.T., Marín-Spiotta, E., 2014. Soil burial contributes to deep soil organic carbon storage. Soil Biology and Biochemistry 69, 251–264.
Cleveland, C.C., Liptzin, D., 2007. C: N:P stoichiometry in soil: is there a "Redfield ratio" for the microbial biomass? Biogeochemistry 85, 235–252.
Craine, J.M., Morrow, C., Fierer, N., 2007. Microbial nitrogen limitation increases decomposition. Ecology 88, 2105–2113.
Ding, B., Li, Z., Qin, Y., 2017. Nitrogen loss from anaerobic ammonium oxidation coupled to Iron (III) reduction in a riparian zone. Environmental Pollution 231, 379–386.
Downes, M., 1978. An improved hydrazine reduction method for the automated determination of low nitrate levels in freshwater. Water Research 12, 673–675.
Dungait, J.A.J., Kemmitt, S.J., Michallon, L., Guo, S., Wen, Q., Brookes, P.C., Evershed, R.P., 2011. Variable responses of the soil microbial biomass to trace concentrations of ^{13}C-labelled glucose, using ^{13}C-PLFA analysis. European Journal of Soil Science 62, 117–126.
Dungait, J.A.J., Hopkins, D.W.H., Gregory, A.S., Whitmore, A.P., 2012. Soil organic matter is governed by accessibility not recalcitrance. Global Change Biology 18, 1781–1796.
Dungait, J.A.J., Kemmitt, S.J., Michallon, L., Guo, S., Wen, Q., Brookes, P.C., Evershed, R.P., 2013. The variable response of soil microorganisms to trace concentrations of low molecular weight organic substrates of increasing complexity. Soil Biology and Biochemistry 64, 57–64.
Ettema, C.H., Lowrance, R., Coleman, D.C., 1999. Riparian soil response to surface nitrogen input: temporal changes in denitrification, labile and microbial C and N pools, and bacterial and fungal respiration. Soil Biology and Biochemistry 31, 1609–1624.
Federle, T.W., Dobbins, D.C., Thornton-Manning, J.R., Jones, D.D., 1986. Microbial biomass, activity, and community structure in subsurface soils. Groundwater 24, 365–374.
Fontaine, S., Barot, S., Barre, P., Bdioui, N., Mary, B., Rumpel, C., 2007. Stability of organic carbon in deep soil layers controlled by fresh carbon supply. Nature 450, 277–280.
Giesler, R., Lundström, U., 1993. Soil solution chemistry: effects of bulking soil samples. Soil Science Society of America Journal 57, 1283–1288.
Glanville, H., Hill, P., Schnepf, A., Oburger, E., Jones, D., 2016. Combined use of empirical data and mathematical modelling to better estimate the microbial turnover of isotopically labelled carbon substrates in soil. Soil Biology and Biochemistry 94,

154–168.
Gocke, M.I., Huguet, A., Derenne, S., Kolb, S., Dippold, M.A., Wiesenberg, G.L., 2017. Disentangling interactions between microbial communities and roots in deep subsoil. Science of the Total Environment 575, 135–145.
Gonzalez-Quiñones, V., Stockdale, E., Banning, N., Hoyle, F., Sawada, Y., Wherrett, A., Jones, D., Murphy, D., 2011. Soil microbial biomass—interpretation and consideration for soil monitoring. Soil Research 49, 287–304.
Graf-Rosenfellner, M., Cierjacks, A., Kleinschmit, B., Lang, F., 2016. Soil formation and its implications for stabilization of soil organic matter in the riparian zone. Catena 139, 9–18.
Gregory, A.S., Dungait, J.A., Watts, C.W., Bol, R., Dixon, E.R., White, R.P., Whitmore, A.P., 2016. Long-term management changes topsoil and subsoil organic carbon and nitrogen dynamics in a temperate agricultural system. European Journal of Soil Science 67, 421–430.
Gremm, T.J., Kaplan, L., 1998. Dissolved carbohydrate concentration, composition, and bioavailability to microbial heterotrophs in stream water. Clean–Soil, Air, Water 26, 167–171.
Hanke, A., Cerli, C., Muhr, J., Borken, W., Kalbitz, K., 2013. Redox control on carbon mineralization and dissolved organic matter along a chronosequence of paddy soils. European Journal of Soil Science 64, 476–487.
Heitkötter, J., Heinze, S., Marschner, B., 2017. Relevance of substrate quality and nutrients for microbial C-turnover in top- and subsoil of a Dystric Cambisol. Geoderma 302, 89–99.
Hill, B.H., Elonen, C.M., Jicha, T.M., Kolka, R.K., Lehto, L.L.P., Sebestyen, S.D., Seifert-Monson, L.R., 2014. Ecoenzymatic stoichiometry and microbial processing of organic matter in northern bogs and fens reveals a common P-limitation between peatland types. Biogeochemistry 120, 203–224.
Hoffmann, T., Mudd, S.M., van Oost, K., Verstraeten, G., Erkens, G., Lang, A., Middelkoop, H., Boyle, J., Kaplan, J.O., Willenbring, J., Aalto, R., 2013. Short Communication: humans and the missing C-sink: erosion and burial of soil carbon through time. Earth Surface Dynamics 1, 45–52.
Hoyle, F., Murphy, D., 2007. Microbial response to the addition of soluble organic substrates. Soil Research 45, 559–567.
Hoyle, F., Murphy, D., Brookes, P., 2008. Microbial response to the addition of glucose in low-fertility soils. Biology and Fertility of Soils 44, 571–579.
Huang, W., Hall, S.J., 2017. Elevated moisture stimulates carbon loss from mineral soils by releasing protected organic matter. Nature Communications 8, 1774.
Jansen, B., Kalbitz, K., McDowell, W.H., 2014. Dissolved organic matter: linking soils and aquatic systems. Vadose Zone Journal 13.
Jenkinson, D.S., Coleman, K., 2008. The turnover of organic carbon in subsoils. Part 2. Modelling carbon turnover. European Journal of Soil Science 59, 400–413.
Jenkinson, D.S., Poulton, P.R., Bryant, C., 2008. The turnover of organic carbon in subsoils. Part 1. Natural and bomb radiocarbon in soil profiles from the Rothamsted long-term field experiments. European Journal of Soil Science 59, 391–399.
Jobbágy, E.G., Jackson, R.B., 2000. The vertical distribution of soil organic carbon and its relation to climate and vegetation. Ecological Applications 10, 423–436.
Jones, D., Kemmitt, S., Wright, D., Cuttle, S., Bol, R., Edwards, A., 2005. Rapid intrinsic rates of amino acid biodegradation in soils are unaffected by agricultural management strategy. Soil Biology and Biochemistry 37, 1267–1275.
Jones, D., Willett, V., 2006. Experimental evaluation of methods to quantify dissolved organic nitrogen (DON) and dissolved organic carbon (DOC) in soil. Soil Biology and Biochemistry 38, 991–999.
Jones, D.L., Magthab, E.A., Gleeson, D.B., Hill, P.W., Sánchez-Rodríguez, A.R., Roberts, P., Ge, T., Murphy, D.V., 2018. Microbial competition for nitrogen and carbon is as intense in the subsoil as in the topsoil. Soil Biology and Biochemistry 117, 72–82.
Jones, D.L., Rousk, J., Edwards-Jones, G., DeLuca, T.H., Murphy, D.V., 2012. Biochar-mediated changes in soil quality and plant growth in a three year field trial. Soil Biology and Biochemistry 45, 113–124.
Keiluweit, M., Gee, K., Denney, A., Fendorf, S., 2018. Anoxic microsites in upland soils dominantly controlled by clay content. Soil Biology and Biochemistry 118, 42–50.
Keller, J.K., Bridgham, S.D., 2007. Pathways of anaerobic carbon cycling across an ombrotrophic-minerotrophic peatland gradient. Limnology and Oceanography 52, 96–107.
Keller, J.K., Wade, J., 2018. No evidence for trace metal limitation on anaerobic carbon mineralization in three peatland soils. Geoderma 314, 95–101.
Kemmitt, S., Lanyon, C., Waite, I., Wen, Q., Addiscott, T., Bird, N.R., O'donnell, A., Brookes, P., 2008a. Mineralization of native soil organic matter is not regulated by the size, activity or composition of the soil microbial biomass—a new perspective. Soil Biology and Biochemistry 40, 61–73.
Kemmitt, S.J., Wright, D., Murphy, D.V., Jones, D.L., 2008b. Regulation of amino acid biodegradation in soil as affected by depth. Biology and Fertility of Soils 44, 933–941.
Kirkby, C.A., Richardson, A.E., Wade, L.J., Batten, G.D., Blanchard, C., Kirkegaard, J.A., 2013. Carbon-nutrient stoichiometry to increase soil carbon sequestration. Soil Biology and Biochemistry 60, 77–86.
Kramer, C., Gleixner, G., 2008. Soil organic matter in soil depth profiles: distinct carbon preferences of microbial groups during carbon transformation. Soil Biology and Biochemistry 40, 425–433.
Kramer, S., Marhan, S., Haslwimmer, H., Ruess, L., Kandeler, E., 2013. Temporal variation in surface and subsoil abundance and function of the soil microbial community in an arable soil. Soil Biology and Biochemistry 61, 76–85.
Lair, G.J., Zehetner, F., Hrachowitz, M., Franz, N., Maringer, F.-J., Gerzabek, M.H., 2009. Dating of soil layers in a young floodplain using iron oxide crystallinity. Quaternary Geochronology 4, 260–266.
Marín-Spiotta, E., Gruley, K.E., Crawford, J., Atkinson, E.E., Miesel, J.R., Greene, S., Cardona-Correa, C., Spencer, R.G.M., 2014. Paradigm shifts in soil organic matter research affect interpretations of aquatic carbon cycling: transcending disciplinary and ecosystem boundaries. Biogeochemistry 117, 279–297.
Marschner, B., Kalbitz, K., 2003. Controls of bioavailability and biodegradability of dissolved organic matter in soils. Geoderma 113, 211–235.
Met Office, 2017. Climate summaries. http://www.metoffice.gov.uk/climate/uk/summaries/datasets, Accessed date: 14 June 2017.
Morel, B., Durand, P., Jaffrezic, A., Gruau, G., Molénat, J., 2009. Sources of dissolved organic carbon during stormflow in a headwater agricultural catchment. Hydrological Processes 23, 2888–2901.
Müller, K., Kramer, S., Haslwimmer, H., Marhan, S., Scheunemann, N., Butenschön, O., Scheu, S., Kandeler, E., 2016. Carbon transfer from maize roots and litter into bacteria and fungi depends on soil depth and time. Soil Biology and Biochemistry 93, 79–89.
Mulvaney, R., 1996. Nitrogen—inorganic Forms. Methods of Soil Analysis Part 3—Chemical Methods. Soil Science Society of America, Madison,WI, pp. 1123–1184.
Murphy, J., Riley, J.P., 1962. A modified single solution method for the determination of phosphate in natural waters. Analytica Chimica Acta 27, 31–36.
Ng, E.L., Patti, A.F., Rose, M.T., Schefe, C.R., Wilkinson, K., Cavagnaro, T.R., 2014. Functional stoichiometry of soil microbial communities after amendment with stabilised organic matter. Soil Biology and Biochemistry 76, 170–178.
Orme, L.C., Charman, D.J., Reinhardt, L., Jones, R.T., Mitchell, F.J., Stefanini, B.S., Barkwith, A., Ellis, M.A., Grosvenor, M., 2017. Past changes in the North Atlantic storm track driven by insolation and sea-ice forcing. Geology 45, 335–338.
Paul, E.A., Clark, F.E., 1996. Soil Microbiology and Biochemistry, second ed. Academic Press, New York.
Poblador, S., Lupon, A., Sabaté, S., Sabater, F., 2017. Soil water content drives spatio-temporal patterns of CO_2 and N_2O emissions from a Mediterranean riparian forest soil. Biogeosciences 14, 4195.
Qualls, R.G., Haines, B.L., 1992. Biodegradability of dissolved organic matter in forest throughfall, soil solution, and stream water. Soil Science Society of America Journal 56, 578–586.
Raymond, P.A., Bauer, J.E., 2001. Use of 14 C and 13 C natural abundances for evaluating riverine, estuarine, and coastal DOC and POC sources and cycling: a review and synthesis. Organic Geochemistry 32, 469–485.
Regnier, P., Friedlingstein, P., Ciais, P., Mackenzie, F.T., Gruber, N., Janssens, I.A., Laruelle, G.G., Lauerwald, R., Luyssaert, S., Andersson, A.J., Arndt, S., Arnosti, C., Borges, A.V., Dale, A.W., Gallego-Sala, A., Goddéris, Y., Goossens, N., Hartmann, J., Heinze, C., Ilyina, T., Joos, F., LaRowe, D.E., Leifeld, J., Meysman, F.J.R., Munhoven, G., Raymond, P.A., Spahni, R., Suntharalingam, P., Thullner, M., 2013. Anthropogenic perturbation of the carbon fluxes from land to ocean. Nature Geoscience 6, 597–607.
Rumpel, C., Kögel-Knabner, I., 2010. Deep soil organic matter—a key but poorly understood component of terrestrial C cycle. Plant and Soil 338, 143–158.
Salomé, C., Nunan, N., Pouteau, V., Lerch, T.Z., Chenu, C., 2010. Carbon dynamics in topsoil and in subsoil may be controlled by different regulatory mechanisms. Global Change Biology 16, 416–426.
Sanaullah, M., Chabbi, A., Maron, P.-A., Baumann, K., Tardy, V., Blagodatskaya, E., Kuzyakov, Y., Rumpel, C., 2016. How do microbial communities in top- and subsoil respond to root litter addition under field conditions? Soil Biology and Biochemistry 103, 28–38.
Sandford, R.C., Hawkins, J.M., Bol, R., Worsfold, P.J., 2013. Export of dissolved organic carbon and nitrate from grassland in winter using high temporal resolution, in situ UV sensing. Science of the Total Environment 456–457, 384–391.
Saunders, W., Williams, E., 1955. Observations on the determination of total organic phosphorus in soils. European Journal of Soil Science 6, 254–267.
Simm, D.J., Walling, D.E., 1998. Lateral variability of overbank sedimentation on a Devon flood plain. Hydrological Sciences Journal 43, 715–732.
Sinsabaugh, R.L., Manzoni, S., Moorhead, D.L., Richter, A., 2013. Carbon use efficiency of microbial communities: stoichiometry, methodology and modelling. Ecology Letters 16, 930–939.
Tipping, E., Somerville, C.J., Luster, J., 2016. The C: N:P: S stoichiometry of soil organic matter. Biogeochemistry 130, 117–131.
Torres-Sallan, G., Schulte, R.P., Lanigan, G.J., Byrne, K.A., Reidy, B., Simo, I., Six, J., Creamer, R.E., 2017. Clay illuviation provides a long-term sink for C sequestration in subsoils. Scientific Reports 7, 45635.
Valett, H., Baker, M., Morrice, J., Crawford, C., Molles, M., Dahm, C.N., Moyer, D., Thibault, J., Ellis, L.M., 2005. Biogeochemical and metabolic responses to the flood pulse in a semiarid floodplain. Ecology 86, 220–234.
von Lützow, M., Kögel-Knabner, I., Ekschmitt, K., Flessa, H., Guggenberger, G., Matzner, E., Marschner, B., 2007. SOM fractionation methods: relevance to functional pools and to stabilization mechanisms. Soil Biology and Biochemistry 39, 2183–2207.
Walling, D., Bradley, S.B., 1989. Rates and patterns of contemporary floodplain sedimentation: a case study of the River Culm, Devon, UK. GeoJournal 19, 53–62.
Walling, D., Fang, D., Nicholas, A., Sweet, R., 2006. River Flood Plains as Carbon Sinks, vol. 306. IAHS Publication, pp. 460.
Wang, J., Dokohely, M.E., Xiong, Z., Kuzyakov, Y., 2015. Contrasting effects of aged and fresh biochars on glucose-induced priming and microbial activities in paddy soil. Journal of Soils and Sediments 16, 191–203.
Wang, Z., Van Oost, K., Lang, A., Quine, T., Clymans, W., Merckx, R., Notebaert, B., Govers, G., 2014. The fate of buried organic carbon in colluvial soils: a long-term perspective. Biogeosciences 11, 873–883.
Wordell-Dietrich, P., Don, A., Helfrich, M., 2017. Controlling factors for the stability of subsoil carbon in a dystric cambisol. Geoderma 304, 40–48.
Worrall, F., Harriman, R., Evans, C.D., Watts, C.D., Adamson, J., Neal, C., Tipping, E., Burt, T., Grieve, I., Monteith, D., 2004. Trends in dissolved organic carbon in UK rivers and lakes. Biogeochemistry 70, 369–402.
Zehetner, F., Lair, G.J., Gerzabek, M.H., 2009. Rapid carbon accretion and organic matter pool stabilization in riverine floodplain soils. Global Biogeochemical Cycles 23.